

Detecting molecular folding from noise measurements

Marc Rico-Pasto¹ and Felix Ritort^{2,3}

¹Unit of Biophysics and Bioengineering, Department of Biomedicine, School of Medicine and Health Sciences, University of Barcelona, C/Casanoves 143, 08036 Barcelona, Spain

²Small Small Biosystems Lab, Condensed Matter Physics Department, Physics School, University of Barcelona, C/Martí i Franquès 1, 08028 Barcelona, Spain

³Institut de Nanociència i Nanotecnologia (IN2UB), University of Barcelona, 08028 Barcelona, Spain

September 13, 2023

Abstract

Detecting conformational transitions in molecular systems is key to understanding biological processes. Here we investigate the force variance in single-molecule pulling experiments as an indicator of molecular folding transitions. We consider cases where Brownian force fluctuations are large, masking the force rips and jumps characteristic of conformational transitions. We compare unfolding and folding data for DNA hairpin systems of loop sizes 4,8, and 20 and the 110 amino acids protein barnase, finding conditions that facilitate the detection of folding events at low forces where the signal-to-noise ratio is low. In particular, we discuss the role of temperature as a useful parameter to improve the detection of folding transitions in entropically driven processes where folding forces are temperature independent. The force variance approach might be extended to detect the elusive intermediate states in RNA and protein folding.

1 Introduction

Protein folding remains a challenging topic in biophysics. In 1968 Levinthal argued that stochastic dif-

usive motion alone could not account for the short timescales of protein folding [1]. Folding a protein into its native structure can be likened to finding a needle in a haystack. Assuming that the backbone dihedral angles of the amino acids chain are divided into three distinct regions of the Ramachandran plot, the typical folding time grows like $3^N \times \tau_d$, with N the number of amino acids and τ_d the diffusive time in such regions. The latter can be expressed as $\tau_d = l^2/6D$, where l is the region size, and D is the diffusion constant. Taking $l \sim 3 \text{ \AA}$, the inter amino-acid distance, and using the Stokes formula $D = k_B T / \gamma$ with $\gamma = 6\pi\eta l$ and $\eta \sim 0.001 \text{ Pa}\cdot\text{s}$ the shear viscosity of water, we obtain $\tau_d = 2 \cdot 10^{-11} \text{ s}$. Thus, a protein consisting of $N = 20$ residues would fold in approximately one second, while for $N = 60$, the folding time would be the universe's age. This rough estimation emphasizes natural evolution's role in speeding up protein folding.

To solve Levinthal's paradox, the molten globule hypothesis was proposed by Ptitsyn in the 70s: native folding is guided by the accumulation of native-like interactions and the sequential formation of intermediates. In small globular proteins, the molten globule is an intermediate between the unfolded and native states, where the polypeptide chain pre-forms a scaffold of the native structure. Experimental measure-

ments suggest a dry molten globule with the outer layer of the protein hydrated and the core dehydrated. The latter has a native-like expanded structure with the backbone formed but with side chains loosely packed [2, 3, 4]. The evidence in favor of molten globule intermediates has always been indirect [5, 6, 7].

The study of protein folding has traditionally relied on bulk experiments such as calorimetry, hydrogen exchange, NMR, and fluorescence spectroscopy. However, these methods have limitations in detecting short-lived intermediates, whose presence is masked by the averaging effect of bulk assays. Single-molecule force spectroscopy experiments have revolutionized the study of protein folding thanks to their unprecedented spatial and temporal resolution, allowing us to detect previously undetectable short-lived intermediates. Recently, using single-molecule experiments it has been demonstrated that the rupture force variance of the ligand-protein complex biotin-streptavidin increases close to the transition state [8]. Optical tweezers have proven especially adept at spotting these intermediates [9, 10, 11, 12], and in co-translational folding assays upon exiting the ribosome [13]. A major twist in experiments has been recently achieved with calorimetric force spectroscopy [14, 15] by measuring the folding enthalpy, entropy, and heat capacity change of the small globular protein barnase [16]. Barnase is a 110 amino acids bacterial ribonuclease protein secreted by the bacterium *Bacillus amyloliquefaciens* and the focus of many studies of protein folding [17, 18, 19, 20]. In reference [21] we found that barnase folds in a two-state manner without observable intermediates at kHz sampling rates. In a subsequent study [22], we demonstrated that the transition state has the thermodynamic properties of a dry molten globule: a native-like structure of high-energy and low configurational entropy relative to the native state. This study also set a thermodynamic ground on the energy landscape hypotheses (ELH) proposed by Wolynes and collaborators in the 80s. In the ELH, proteins fold along a funnel-shaped energy landscape with multiple productive folding trajectories [23, 24].

Despite the many studies on barnase, direct observation of the hypothesized molten globule inter-

mediate has not been possible. A major question is identifying experimental limitations to detect hidden short-lifetime states using noise force measurements. Here we address noise measurements of the unfolding and folding dynamics of barnase measured in pulling experiments at different temperatures (7-37°C) [22]. We compare such measurements with those obtained in DNA hairpins of varying loop sizes, where the entropic barrier to folding is large, like for proteins. To this end, we measured the force variance in pulling experiments at loading rates 4–7pN/s and 1kHz sampling rate. We ask whether folding events can be detected in an entropy-driven process where folding forces are low, and the folding rip is indistinguishable from the noise. We also analyze the effect of decreasing temperature to reduce thermal fluctuations and increase the signal-to-noise ratio of the folding events. Detecting folding events is critical to identify folding intermediates that require additional resolution in the experiments. Here we will focus on detecting folding events in DNA hairpins and barnase, setting the basis for future studies for detecting the often elusive folding intermediates.

2 Materials and methods

In pulling experiments with optical tweezers, the molecule under study (DNA hairpins and barnase) is tethered between two beads. Double-stranded DNA (dsDNA) handles are attached to the end of the molecule to prevent nonspecific interactions between molecules and beads. The handles are ligated to the N- and C-termini for protein barnase via cysteine-thiol chemical reduction (details in Ref.[21]). For the DNA hairpins, designed oligos are hybridized and ligated to build a DNA construct consisting of the hairpin and two flanking 29bp short handles (details in Ref. [25]). The 5'- end of the molecular construct is attached to one bead via anti-digoxigenin - digoxigenin bonds (3.0 to 3.4 μm diameter counts; Spherotech, Libertyville, IL), while the other end is attached to a micron-sized polystyrene microsphere using streptavidin-biotin bonds (2.0 to 2.9 μm diameter bead; G. Kisker Biotech, Steinfurt, Germany). The first bead is captured in the optical trap to mea-

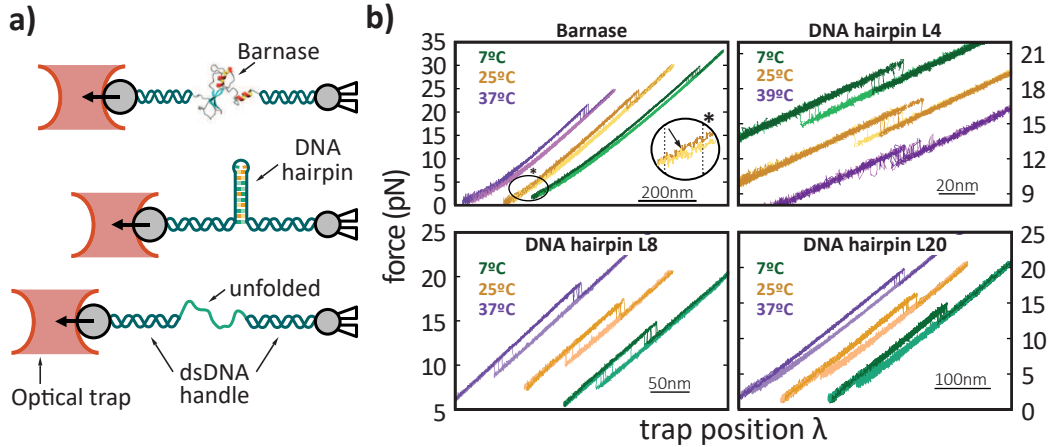


Figure 1: a) Experimental setup. Barnase and DNA hairpins are tethered between two polystyrene beads through two dsDNA handles. One bead is fixed by air suction at the tip of a micro-pipette, while the optical trap controls the other. b) Force-distance curves (FDCs) for barnase (top, left), the DNA hairpin L4 (top, right), hairpin L8 (bottom, left), and hairpin L20 (bottom, right) measured at 7°C (green), 25°C (orange), and 37-39°C (purple). The dark color lines denote the unfolding trajectories, while the light color lines correspond to folding trajectories. In the starred ellipse, it is highlighted a folding event for barnase at 25°C.

sure the force, while the other is immobilized at the tip of a micro-pipette by air suction (Fig. 1a).

In a pulling experiment, a molecule is tethered between two beads, and the optical trap is moved between a minimum force where the molecule is folded and a maximum force where it is unfolded. In a pulling cycle, the force applied to the system increases (decreases) when moving the optical trap away (towards) the pipette. To change the temperature, we use the temperature-jump optical trap described in Ref.[14], where an extra collimated laser is used to heat the medium surrounding the optical trap uniformly. For low-temperature measurements, the instrument is put inside an icebox kept at 4°C, permitting us to do measurements in the range of 4-40°C.

3 Results and discussion

The force is repeatedly stretched and released in pulling experiments while recording the force versus trap-position distance curves (FDCs). In the unfold-

ing process, a force rip is observed at high forces (> 15pN), indicating the transition from the native (N) to the unfolded (U) state (dark color trajectories in Fig.1b). Furthermore, the value of force where the transition is observed varies from one pull to another, indicating that the unfolding events are thermally activated. In the refolding process, the force is reduced until a folding event is observed as a sudden force rise. The size of the force jump is proportional to the difference in molecular extension between N and U . However, as can be seen in Fig.1b (light color trajectories), a rise in the force cannot be appreciated in the folding FDCs of barnase because the folding event takes place at low forces, < 5pN. At such low forces, the magnitude of the force jump is expected to be comparable to the noise.

To detect the folding transition, we measured the variance of the force signal in the unfolding and folding trajectories separately. The analysis of the force variance considers the effects due to the bead, handles, and molecule under study that are modeled as three serially connected springs. The optical trap is

modeled using Hooke's law,

$$f = k_b x_b \quad (1)$$

where f is the force, k_b is the stiffness of the optical trap, and x_b is the displacement of the bead to the trap's center. The dsDNA handles, and the unfolded state of the DNA hairpin and barnase are modeled with the Worm-Like Chain (WLC) model [26],

$$f = \frac{k_B T}{4L_p} \left(\left(1 - \frac{x}{L_c}\right)^{-2} + 4\frac{x}{L_c} - 1 \right). \quad (2)$$

In Eq.(2), k_B is the Boltzmann constant, T is the temperature, x is the extension of the molecule, and L_c is the contour length of the handles or the unfolded molecule. Extensibility is considered for the case of the short dsDNA handles in the DNA hairpins case, by correcting the extension x with the term $(1+f/Y)$ where $Y = 16pN$ for the 29bp dsDNA handles [25]. Finally, the elastic response of the folded molecule is modeled as a dipole oriented under an applied force. Its extension is modeled with the Freely-Jointed Chain model (FJC),

$$x = d_0 \left(\coth \left(\frac{d_0 f}{k_B T} \right) - \frac{k_B T}{d_0 f} \right). \quad (3)$$

In Eq.(3), x is the dipole extension at force f , d_0 is the dipole contour length, which is equal to 2nm for the DNA hairpin, and 3nm for barnase.

3.1 Force variance in a two-branches model

In our pulling experiments, the control parameter is the trap position λ , and the measured force is a fluctuating quantity. To detect the folding transitions we compute the force variance (σ_f^2) in a statistical model with two branches, folded and unfolded, describing the experimental FDCs shown in Fig. 1. The upper and lower branches in the FDCs of Fig. 1b stand for the folded (N) and unfolded (U) branches where the molecule is in the Native (N) or Unfolded (U) states showing distinct FDCs. In what follows, force branches and states are used indistinctly: folded branch \leftrightarrow N and unfolded branch \leftrightarrow U . In equilibrium,

the probability of observing the molecule in states N or U (P_N and P_U) is given by the Boltzmann-Gibbs factor:

$$P_{N(U)} = \frac{\exp\left(\frac{-\Delta G_{N(U)}}{k_B T}\right)}{Z_\lambda} \quad (4)$$

where $\Delta G_{N(U)}$ is the partial free energy of $N(U)$ at a given trap position and $Z_\lambda = \exp(-\Delta G_N/k_B T) + \exp(-\Delta G_U/k_B T)$ is the partition function of the system (molecule, handles, and bead). The partial free energy of the system when the molecule (DNA hairpins and barnase) is in N and U is calculated as:

$$\begin{aligned} \Delta G_N &= \int_0^{x_d} f_d(x') dx' + \int_0^{x_h^N} f_h(x') dx' \\ &+ \int_0^{x_b^N} f_b(x') dx'. \end{aligned} \quad (5a)$$

$$\begin{aligned} \Delta G_U &= \Delta G_0 + \int_0^{x_U} f_U(x') dx' + \int_0^{x_h^U} f_h(x') dx' \\ &+ \int_0^{x_b^U} f_b(x') dx'. \end{aligned} \quad (5b)$$

where x_d denotes the projected extension of the dipole, x_U is the extension of the unfolded molecule, $x_h^{N(U)}$ is the extension of the handles, and $x_b^{N(U)}$ is the bead displacement, all quantities evaluated at the force when the molecule is in N or U (i.e., $x_b^N := x_b(f_U)$; $x_b^U := x_b(f_U)$). The forces acting on each element are defined as f_d (dipole), f_h (handles), f_b (beads), f_U (unfolded polymer) and have different elastic responses resulting in the observed different force branches of Figure 1b. These relations have been defined in Eqs. (1),(2),(3). Note that f_d, f_h, f_b, f_U are equal at the upper integration limits in (5a) and in (5b), corresponding to serially connected springs.

In the absence of force jumps between the two branches, the force variance is given by,

$$\sigma_f^2 = P_N \sigma_f^2(N) + P_U \sigma_f^2(U) \quad (6)$$

The force variances in each branch, $\sigma_f^2(N)$ and $\sigma_f^2(U)$, are determined by the elastic properties of the molecular construct in that branch, $k_m(N), k_m(U)$,

$$\sigma_f^2(N, U) = \frac{k_B T k_b^2}{k_b + k_m(N, U)} \quad (7)$$

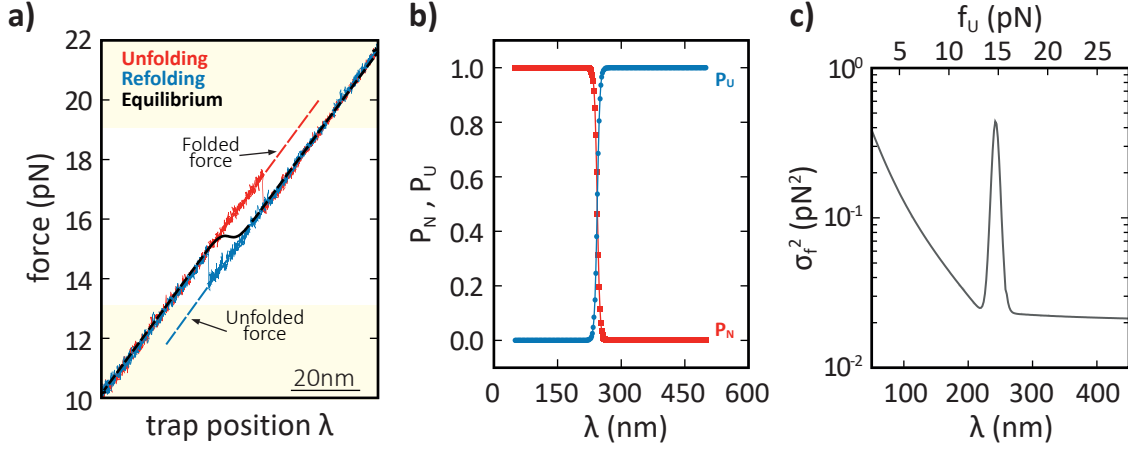


Figure 2: Force variance calculation Eq.(14). a) Unfolding (red) and folding (blue) FDCs measured for the DNA hairpin L4 at 25°C. The red and blue dashed lines denote the folded and unfolded force branches. The black line is the calculated equilibrium FDC. b) Equilibrium probability of the native (P_N ,red) and unfolded (P_U ,blue) as a function of the trap position λ . c) Theoretically predicted σ_f^2 for DNA hairpin L4 at 25°C as a function of trap position (λ ,bottom x-axis) and force in the unfolded branch (f_U ,top x-axis).

where $1/k_m(N) = 1/k_h + 1/k_d$ and $1/k_m(U) = 1/k_h + 1/k_U$ is the stiffness of the molecular construct, resulting from two serially connected springs of stiffnesses k_h (handle) and k_d (dipole for the folded state) or k_U for the unfolded polymer. k_U and k_d are derived from Eq.(2) and Eq.(3), respectively.

At a given trap position λ , the equilibrium force $\langle f \rangle$ and its second moment $\langle f^2 \rangle$ are defined as:

$$\langle f \rangle = \frac{1}{Z_\lambda} \left(\langle f_N \rangle e^{-\Delta G_N/k_B T} + \langle f_U \rangle e^{-\Delta G_U/k_B T} \right) \quad (8a)$$

$$\langle f^2 \rangle = \frac{1}{Z_\lambda} \left(\langle f_N^2 \rangle e^{-\Delta G_N/k_B T} + \langle f_U^2 \rangle e^{-\Delta G_U/k_B T} \right) \quad (8b)$$

where $\langle f_{N(U)} \rangle$ denotes the average force when the molecule is in $N(U)$, i.e., $\langle f_{N(U)} \rangle = \partial_\lambda \Delta G_{N(U)}$ with $\Delta G_{N(U)}$ given in Eqs. (5a),(5b).

To determine the variance of the force, we calculated the second derivative of the thermodynamic po-

tential $\Delta G(\lambda)$:

$$\Delta G(\lambda) = -k_B T \log(Z_\lambda) \quad (9a)$$

$$\langle f \rangle = \partial_\lambda \Delta G(\lambda) \quad (9b)$$

$$\partial_\lambda^2 \Delta G(\lambda) = \partial_\lambda \langle f \rangle = k_{eff} \quad (9c)$$

where k_{eff} is the effective stiffness of the system along the equilibrium FDC. Using the definition of $\langle f \rangle$ Eq. (8a) we compute $\partial_\lambda \langle f \rangle$:

$$\partial_\lambda \langle f \rangle = A(\lambda) \cdot \partial_\lambda \left(\frac{1}{Z_\lambda} \right) + \frac{1}{Z_\lambda} \cdot \partial_\lambda (A(\lambda)) \quad (10)$$

with $A(\lambda) = \langle f_N \rangle e^{-\Delta G_N/k_B T} + \langle f_U \rangle e^{-\Delta G_U/k_B T}$. For the first term $A(\lambda) \cdot \partial_\lambda (1/Z_\lambda)$, we use the definition of Z_λ in Eqs. (9a),(9b):

$$A(\lambda) \cdot \partial_\lambda \left(\frac{1}{Z_\lambda} \right) = -\frac{A(\lambda)}{Z_\lambda} \cdot \partial_\lambda (\log Z_\lambda) = \frac{\langle f \rangle^2}{k_B T} \quad (11)$$

where we used $\langle f \rangle = A(\lambda)/Z_\lambda$. The second term, $1/Z_\lambda \cdot \partial_\lambda (A(\lambda))$, is obtained by taking the λ -derivative of the above definition for $A(\lambda)$, and using $\langle f^2 \rangle$ in Eq. (8b):

$$\frac{1}{Z_\lambda} \partial_\lambda A(\lambda) = \langle k \rangle - \frac{\langle f^2 \rangle + P_N \sigma_f^2(N) + P_U \sigma_f^2(U)}{k_B T} \quad (12)$$

where,

$$\langle k \rangle = \frac{1}{Z_\lambda} \left(\langle k_N \rangle e^{-\Delta G_N/k_B T} + \langle k_U \rangle e^{-\Delta G_U/k_B T} \right), \quad (13)$$

is the equilibrium stiffness and $\langle k_{N(U)} \rangle = \partial_\lambda \langle f_{N(U)} \rangle$, are the stiffnesses of each branch, equal to the slope in the corresponding force branch (N or U). Introducing Eqs. (11) and (12) into Eq. (10) and using (4), and (9c), we get:

$$\sigma_f^2 = k_B T (\langle k \rangle - k_{eff}) + P_N \sigma_f^2(N) + P_U \sigma_f^2(U) \quad (14)$$

with $\sigma_f^2 = \langle f^2 \rangle - \langle f \rangle^2$ the force variance of the equilibrium FDC and $\sigma_f^2(N, U) = \langle f^2(N, U) \rangle - \langle f(N, U) \rangle^2$ the variance force for each branch, Eq.(7). Notice that, $\sigma_f^2(N, U)$ differs from $k_B T \langle k_{N(U)} \rangle$. For one branch only, e.g. $P_N = 1, P_U = 0$ we get $\langle k \rangle = k_{eff} = \langle k_N \rangle$ and $\sigma_f^2 = \sigma_f^2(N)$. In general, for systems with two branches, the slope of the FDC becomes negative in the region where the two branches coexist $P_N \sim P_U \sim 1/2$ and k_{eff} can become negative (black line connecting the two branches in Fig.2a).

Figure 2a shows an experimental unfolding (red curve) and folding (blue curve) trajectory measured for DNA hairpin L4. Notice that at low (high) force values, $f < 13$ ($f > 19$) pN, the unfolding and folding trajectories overlap onto the folded (unfolded) branches (dashed lines), respectively. In between, unfolding and folding transitions are observed as red force rips and blue force jumps in Fig. 2a. To construct the equilibrium FDC (black line in Fig. 2a), we define the native and unfolded force branches at low and high forces outside the region limited by the force rips and jumps (red and blue dashed lines). The force branches have been calculated by fitting the elastic properties of the optical trap (k_b), by imposing the previously determined elastic properties of handles and unfolded polymers [25, 22, 27] and their folding free energies [28, 22]. This permits us to determine $\sigma_f^2(N), \sigma_f^2(U)$ from Eq.(7) and P_N, P_U from Eq.(4). Equilibrium probabilities for each branch (red, folded; blue, unfolded) are shown in Fig. 2b. We derive σ_f^2 in (14) by computing $\langle k \rangle$ from the equilibrium FDC, and the effective stiffness of each force branch, $\langle k_N \rangle$ and $\langle k_U \rangle$. Figure 2c shows the estimated σ_f^2 for the DNA hairpin L4 at 25°C as a func-

tion of the trap position (bottom axis) and the force in the unfolded branch (top axis). As expected, σ_f^2 decreases with force at low forces (F branch) and high forces (U branch) but shows a peak at the transition region $f_U \sim 15pN$ due to the contribution of the term k_{eff} in (14).

The above calculations can be extended for systems with more than two branches. The average stiffness is given by:

$$\langle k \rangle = (1/Z_\lambda) \sum_{m=0}^M \partial_\lambda f_m \exp(-\Delta G_m/k_B T), \quad (15)$$

with M the total number of branches and $Z_\lambda = \sum_{m=0}^M \exp(-\Delta G_m/k_B T)$. Measuring $\langle k \rangle$ and k_{eff} in equilibrium might detect intermediates by fitting the data to theoretical predictions for $M = 2, 3, \dots$. However, our pulling experiments are out of equilibrium, so the equilibrium prediction cannot be directly used to investigate the hypothesized intermediate state in barnase.

3.2 DNA hairpins

The experimental values of σ_f^2 for DNA hairpins were extracted from the experimental FDCs measured at loading rates of 4–6 pN/s by averaging the force signal in λ -windows of 10nm, meaning that the force increases/decreases $\sim 0.5pN$ inside each window. Figure 3a shows the measured σ_f^2 along the unfolding (red) and folding (blue) process for the DNA hairpin L4 at 7°C (top), 25°C (center), and 37°C (bottom) as a function of the force at the unfolded force branch, f_U . We remark four features from Figure 3a: first, the σ_f^2 values overlap at high and low forces as expected because the molecular state is the same (folded or unfolded). Second, the forces at which σ_f^2 is maximum (unfolding, red; folding, blue) shift to lower values as temperature increases. Third, the hysteresis of σ_f^2 between unfolding (red) and folding (blue) decreases with temperature. Fourth, equilibrium transitions are expected to populate forces between the two maxima. In fact, at 39°C the measured unfolding (red) and folding (blue) σ_f^2 match the equilibrium prediction (black line) because experiments

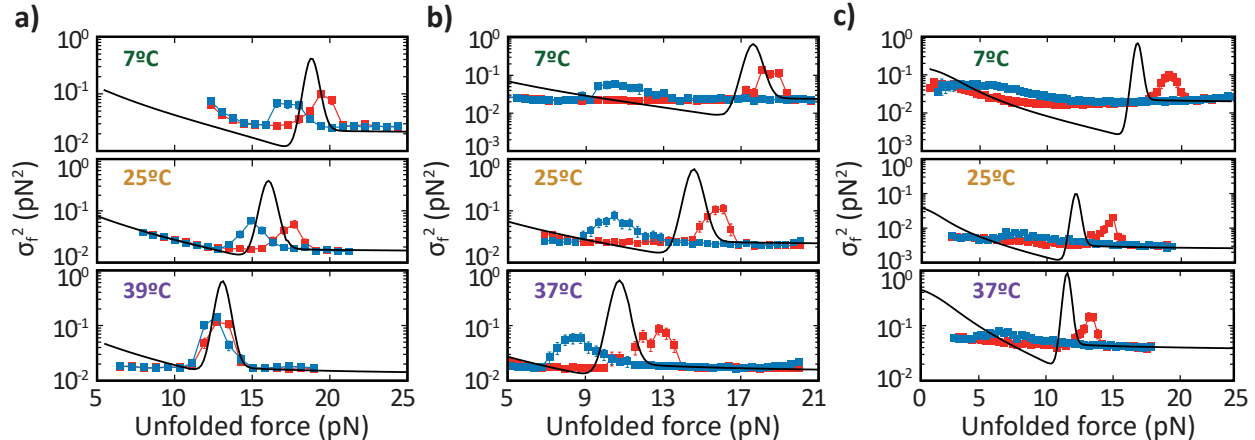


Figure 3: Force variance σ_f^2 for the DNA hairpin L4 (panel a), L8 (panel b), and L20 (panel c) measured at 7°C (top), 25°C (center), and 39°C (bottom) as a function of the measured force along the unfolded force branch. Notice that the unfolding peak of these hairpins takes place at lower forces as we increase the temperature, while the folding peak remains independent of the temperature for L8 and L20.

were carried out under quasi-static conditions (see Fig. 1b top, right).

Regarding the DNA hairpins with loop sizes 8 and 20, we note that σ_f^2 during the unfolding process (red dots in Fig. 3b,c) shifts with temperature, whereas the same data during refolding (blue dots in Fig. 3b,c) change comparably much less with temperature. This is an indication that folding is entropically driven. Notice also that the unfolding forces where σ_f^2 is maximum (red symbols in Fig. 3) are similar for L4, L8, and L12, in agreement with the fact that the transition state of unfolding is located within hairpin’s stem and independent of loop’s size.

3.3 Barnase

For barnase, σ_f^2 was calculated by averaging the force over λ -windows of 8nm in the FDCs. Like for DNA hairpins, σ_f^2 during the folding process (blue points in Fig. 4) changes with temperature comparably much less than the unfolding process (red points in Fig. 4). Figure 4 shows that barnase folds around 4 pN at the three temperatures, while the unfolding events and maximum σ_f^2 occur at 30pN at 7°C, 26pN at 25°C, and 22pN at 37°C.

4 Conclusions

We studied the variance of the force signal, σ_f^2 , in single-molecule pulling experiments. Our aim is to detect entropically driven folding at low forces where the magnitude of force fluctuations is high, and the signal-to-noise ratio of the folding events is low. Moreover, we computed the equilibrium force variance and compared it with the force variance measured in non-equilibrium conditions.

First, we studied three DNA hairpins as toy models to test the method’s validity. The studied hairpins have a stem formed by 20 base pairs and four (L4), eight (L8), and twenty (L20) bases in the loop. The first studied hairpin, L4, has a small entropic barrier to folding, showing folding and unfolding transitions at sufficiently high forces (Fig. 3a). For L4, the force variance σ_f^2 detects the forces at which folding and unfolding transitions occur. We have also observed that the unfolding and folding transitions for L4 are temperature-dependent while the folding transitions for L8 and L20 are roughly temperature-independent indicating that the folding process is entropically driven (Figs. 3b,c).

Next, we studied the folding process of protein bar-

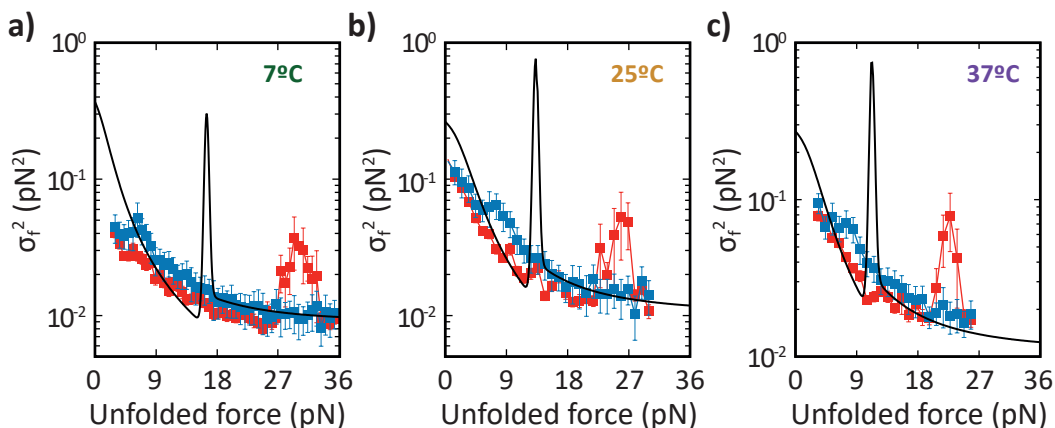


Figure 4: Force variance σ_f^2 for barnase measured at 7°C (panel a), 25°C (panel b), and 37°C (panel c) as a function of the force along the U branch. Notice that the unfolding transition (peak in the red symbols) appears at higher forces as we decrease the temperature, while the folding event (peak in the blue symbols) does not move with temperature.

nase. This transition is challenging to detect in the FDCs (zoom in Fig. 1b), but it is observed as a gentle bump around 4pN in the force variance σ_f^2 (blue squares in Fig. 4). In this case, the transition is not observed as a clear maximum as in the case of DNA hairpins L4 and L8 (blue squares in Fig. 3a,b), because folding occurs far from equilibrium. In fact, the gentle bump observed for either L20 (blue squares in Fig. 3c) and barnase (blue squares in Fig. 4) should become a peak in equilibrium conditions (black lines), demonstrating that folding in these two molecules is highly irreversible. Indeed, hopping transitions between these molecules' folded and unfolded states cannot be observed within the experimentally accessible timescales.

Future work should consider molecular intermediates and the usefulness of measuring the force variance σ_f^2 to detect them. Our approach might be extended by considering a theory for σ_f^2 in out-of-equilibrium conditions where detecting structural transition is challenging.

References

- [1] C. Levinthal, "Are there pathways for protein folding?," *Journal de chimie physique*, vol. 65, pp. 44–45, 1968.
- [2] O. Ptitsyn, "Molten globule and protein folding," vol. 47 of *Advances in Protein Chemistry*, pp. 83–229, Academic Press, 1995.
- [3] G. J. Vidugiris, J. L. Markley, and C. A. Royer, "Evidence for a molten globule-like transition state in protein folding from determination of activation volumes," *Biochemistry*, vol. 34, no. 15, pp. 4909–4912, 1995.
- [4] M. Arai and K. Kuwajima, "Role of the molten globule state in protein folding," *Advances in protein chemistry*, vol. 53, pp. 209–282, 2000.
- [5] G. Semisotnov, N. Rodionova, O. Razgulyaev, V. Uversky, A. Gripas', and R. Gilmanshin, "Study of the "molten globule" intermediate state in protein folding by a hydrophobic fluorescent probe," *Biopolymers: Original Research on Biomolecules*, vol. 31, no. 1, pp. 119–128, 1991.

- [6] C. L. Chyan, C. Wormald, C. M. Dobson, P. A. Evans, and J. Baum, "Structure and stability of the molten globule state of guinea pig. alpha.-lactalbumin: A hydrogen exchange study," Biochemistry, vol. 32, no. 21, pp. 5681–5691, 1993.
- [7] C. Redfield, "Using nuclear magnetic resonance spectroscopy to study molten globule states of proteins," Methods, vol. 34, no. 1, pp. 121–132, 2004. Investigating Protein Folding, Misfolding and Nonnative States: Experimental and Theoretical Methods.
- [8] W. Cai, M. Jäger, J. T. Bullerjahn, T. Hugel, S. Wolf, and B. N. Balzer, "Anisotropic friction in a ligand-protein complex," Nano Letters, 2023.
- [9] C. Cecconi, E. A. Shank, C. Bustamante, and S. Marqusee, "Direct observation of the three-state folding of a single protein molecule," Science, vol. 309, no. 5743, pp. 2057–2060, 2005.
- [10] J. C. M. Gebhardt, T. Bornschlöggl, and M. Rief, "Full distance-resolved folding energy landscape of one single protein molecule," Proceedings of the National Academy of Sciences, vol. 107, no. 5, pp. 2013–2018, 2010.
- [11] P. J. Elms, J. D. Chodera, C. Bustamante, and S. Marqusee, "The molten globule state is unusually deformable under mechanical force," Proceedings of the National Academy of Sciences, vol. 109, no. 10, pp. 3796–3801, 2012.
- [12] K. Neupane, A. P. Manuel, and M. T. Woodside, "Protein folding trajectories can be described quantitatively by one-dimensional diffusion over measured energy landscapes," Nature Physics, vol. 12, no. 7, pp. 700–703, 2016.
- [13] C. M. Kaiser, D. H. Goldman, J. D. Chodera, I. Tinoco, and C. Bustamante, "The ribosome modulates nascent protein folding," Science, vol. 334, no. 6063, pp. 1723–1727, 2011.
- [14] S. de Lorenzo, M. Ribezzi-Crivellari, J. R. Arias-Gonzalez, S. B. Smith, and F. Ritort, "A temperature-jump optical trap for single-molecule manipulation," Biophysical journal, vol. 108, no. 12, pp. 2854–2864, 2015.
- [15] M. Rico-Pasto, I. Pastor, and F. Ritort, "Force feedback effects on single molecule hopping and pulling experiments," The Journal of chemical physics, vol. 148, no. 12, p. 123327, 2018.
- [16] V. A. Mitkevich, A. A. Schulga, Y. S. Ermolyuk, V. M. Lobachov, V. O. Chekhov, G. I. Yakovlev, R. W. Hartley, C. N. Pace, M. P. Kirpichnikov, and A. A. Makarov, "Thermodynamics of denaturation of complexes of barnase and binase with barstar," Biophysical Chemistry, vol. 105, no. 2-3, pp. 383–390, 2003.
- [17] A. Matouschek, J. T. Kellis Jr, L. Serrano, and A. R. Fersht, "Mapping the transition state and pathway of protein folding by protein engineering," Nature, vol. 340, no. 6229, pp. 122–126, 1989.
- [18] A. R. Fersht, "Protein folding and stability: the pathway of folding of barnase," FEBS letters, vol. 325, no. 1-2, pp. 5–16, 1993.
- [19] F. Khan, J. I. Chuang, S. Gianni, and A. R. Fersht, "The kinetic pathway of folding of barnase," Journal of Molecular Biology, vol. 333, no. 1, pp. 169–186, 2003.
- [20] V. A. Mitkevich, A. A. Schulga, Y. S. Ermolyuk, V. M. Lobachov, V. O. Chekhov, G. I. Yakovlev, R. W. Hartley, C. N. Pace, M. P. Kirpichnikov, and A. A. Makarov, "Thermodynamics of denaturation of complexes of barnase and binase with barstar," Biophysical chemistry, vol. 105, no. 2-3, pp. 383–390, 2003.
- [21] A. Alemany, B. Rey-Serra, S. Frutos, C. Cecconi, and F. Ritort, "Mechanical folding and unfolding of protein barnase at the single-molecule level," Biophysical journal, vol. 110, no. 1, pp. 63–74, 2016.
- [22] M. Rico-Pasto, A. Zaltron, S. J. Davis, S. Frutos, and F. Ritort, "Molten globule-like transition

- state of protein barnase measured with calorimetric force spectroscopy,” Proceedings of the National Academy of Sciences, vol. 119, no. 11, p. e2112382119, 2022.
- [23] H. Frauenfelder, S. G. Sligar, and P. G. Wolynes, “The energy landscapes and motions of proteins,” Science, vol. 254, no. 5038, pp. 1598–1603, 1991.
- [24] J. D. Bryngelson, J. N. Onuchic, N. D. Socci, and P. G. Wolynes, “Funnel, pathways, and the energy landscape of protein folding: a synthesis,” Proteins: Structure, Function, and Bioinformatics, vol. 21, no. 3, pp. 167–195, 1995.
- [25] N. Forns, S. de Lorenzo, M. Manosas, K. Hayashi, J. M. Huguette, and F. Ritort, “Improving signal/noise resolution in single-molecule experiments using molecular constructs with short handles,” Biophysical journal, vol. 100, no. 7, pp. 1765–1774, 2011.
- [26] C. Bustamante, J. F. Marko, E. D. Siggia, S. Smith, et al., “Entropic elasticity of lambda-phage dna,” Science, vol. 265, pp. 1599–1599, 1994.
- [27] M. Rico-Pasto and F. Ritort, “Temperature-dependent elastic properties of dna,” Biophysical Reports, vol. 2, no. 3, 2022.
- [28] J. M. Huguette, C. V. Bizarro, N. Forns, S. B. Smith, C. Bustamante, and F. Ritort, “Single-molecule derivation of salt dependent base-pair free energies in dna,” Proceedings of the National Academy of Sciences, vol. 107, no. 35, pp. 15431–15436, 2010.